Identifying the effects of human pressure on groundwater quality to support water management strategies in coastal regions: a multi-tracer and statistical approach (Bou-Areg region, Morocco)

Re V.[1, 2], Sacchi E.[3], Mas-Pla J.[4,5], Menció A.[4], El Amrani N.[6]

[1] Department of Molecular Sciences and Nanosystems, Ca' Foscari University of Venice, Calle Larga Santa Marta 2137 – Dorsoduro 40123 Venice, Italy
email: re@unive.it
Fax: +39 041 234 8591
[2]National Engineering School of Sfax (ENIS) - Laboratory of Radio-Analysis and Environment (LRAE) Sfax, Tunisia
[3]Department of Earth and Environmental Sciences, University of Pavia, Via Ferrata 1, 27100 Pavia, Italy
[4] Grup de Geologia Aplicada i Ambiental (GAIA), Centre de Geologia i Cartografia Ambientals (GEOCAMB), Department of Environmental Sciences, University of Girona. 17071 Girona, Spain
[5] Catalan Institute for Water Research (ICRA), 17003 Girona, Spain
[6] Faculty of Sciences and techniques, University Hassan 1er, Settat, Morocco

Abstract

Groundwater pollution from anthropogenic sources is a serious concern affecting several coastal aquifers worldwide. Increasing groundwater exploitation, coupled with point and non-point pollution sources, are the main anthropogenic impacts on coastal environments and are responsible for severe health and food security issues. Adequate management strategies to protect groundwater from contamination and overexploitation are of paramount importance, especially in arid prone regions, where coastal aquifers often represent the main freshwater resource to sustain human needs.

The Bou-Areg Aquifer (Morocco) is a perfect example of a coastal aquifer constantly exposed to all the negative externalities associated with groundwater use for agricultural purposes, which lead to a general increase in aquifer salinization. In this study data on 61 water samples, collected in June and November 2010, were used to: (i) track groundwater composition changes related to the use of irrigation water from different sources, (ii) highlight seasonal variations to assess aquifer vulnerability, and (iii) present a reproducible example of multi-tracer approach for groundwater management in rural coastal areas.

Hydrogeochemical results show that Bou-Areg groundwater is characterized by - high salinity, associated with a remarkable increase in bicarbonate content in the crop growing season, due to more intense biological activity in irrigated soils. The coupled multi-tracer and statistical analysis confirms the strong dependency on irrigation activities as well as a clear identification of the processes governing the aquifer's hydrochemistry in the different seasons. Water Rock Interaction (WRI) dominates the composition of most of groundwater samples in the Low Irrigation season (L-IR) and Agricultural Return Flow (ARF) mainly affects groundwater salinization in the High Irrigation season (H-IR) in the same areas naturally affected by WRI. In the central part of the plain River Recharge (RR) from the Selouane River is responsible for the high groundwater salinity whilst Mixing Processes (MIX) occur in absence of irrigation activities.

Keywords: stable isotopes, irrigation, human impacts; PCA, MedPartnership; Morocco

1. Introduction

The Mediterranean Basin is among the most arid regions in the world, where limited water resources are unevenly distributed in space and time (GWP, 2013). In particular, southern rim countries are either in arid or hyper-arid zones heavily depending on seasonal rainfall (World Bank, 2007). These regions have few permanent rivers (some of which carry runoff from other countries) and therefore often rely on fragile, and sometimes non-renewable, groundwater resources. As a result, more than 180 million people are considered water poor (i.e., their available amount of water is less than 1000 m^3 of renewable water per capita per year), and an additional 60 million face water stress (i.e., their available amount of water is less than 500 m^3 of renewable water per capita per year; GWP, 2013). The recent demographic growth, with the consequent increasing urbanization, agricultural demand and resource-intensive socioeconomic development, exerts additional pressures on scarce resources and fragile coastal ecosystems (Pereira, 2004). The situation is expected to worsen in the future, due to climate changes strongly impacting on precipitation amount and rainfall type (Navarra and Tubiana, 2013).

Under this pressure, the scientific community recognized the need to better assess the links between water and irrigated agriculture. The emphasis is especially focused on regional and local studies on groundwater suitability for irrigation purposes, resulting in numerous investigations based on different hydrogeochemical tools and indices (e.g. Watanabe et al., 2008; Tadesse et al., 2010; Ravikumar et al., 2011; Romanelli et al., 2012). Nonetheless, studies on the impact of irrigation on groundwater quality are mainly related to the assessment of diffuse pollution impact on groundwater quality, especially associated with fertilizers use and farming activities (e.g. Pionke et al., 1990, El Amrani et al., 2007, Boulabeiz, 2011; Boy-Roura et al., 2013), while relatively fewer report on the impacts of agriculture practices on salinity (e.g. Suarez, 1989; Kass et al., 2005; Qin et al., 2011) and on non-nitrogen contamination (Stigter et al., 2006; Qadir and Oster, 2004; Scanlon et al., 2010; Croon 2013; Oh et al., 2013).

Morocco, as most of the southern rim Mediterranean countries, is a highly water stressed nation with erratic rainfall and frequent droughts (GWP and DBSA, 2012). Under these generalized conditions of physical water scarcity (IWMI, 2007), the current water use patterns and withdrawals are considered unsustainable and water security is becoming a major limiting factor for the socio-economic development of the country (GWP and DBSA, 2012). Among all the productive sectors, agriculture is the largest water user, especially in dry seasons, and at the same time the main source of income for 80% of the rural population and 14-20% of the kingdom's Gross Domestic Product (EMWIS, 2013).

In Morocco, as worldwide, irrigated agriculture has become the predominant groundwater consumer, raising questions about resource sustainability and irreversible degradation, eventually leading to numerous cross-sector policy and management issues (Foster and Ait-Kad, 2012). Indeed, improving agricultural efficiency would allow better allocating water resources and adequately ensuring the access to safe drinking water and food.

The region of Nador (North of Morocco) is a clear example of the aforementioned needs and problems. Groundwater withdrawn from hand dug wells has been traditionally used to sustain agricultural and domestic needs. Overexploitation and pollution from anthropogenic activities (urban, agricultural and industrial) significantly impaired groundwater quality and soil fertility (El Mandour et al. 2008, El Yaouti et al. 2008, El Yaouti et al. 2009).

A preliminary investigation in the coastal aquifer of Bou-Areg and the adjacent lagoon of Nador was conducted to characterize aquifer recharge and salinization processes (Re et al., 2013a). Results showed that recharge is mainly due to mountain runoff, interacting with local recharge sources (ephemeral rivers and irrigation waters) resulting in a complex system of mixed waters. The high salinity of the aquifer was attributed to the coexistence of dissolution processes of evaporative rocks and carbonates, water-rock interaction, and human impacts. Agricultural return flow was identified as the main anthropogenic contribution to groundwater salinization in the central part of the plain, also causing a general increase in nitrate concentrations. Only locally, nearby the coastline, the high salinization was attributed to the presence of lagoon water intrusion.

This work presents a second step for the complete assessment of recharge and pollution processes in the Bou-Areg aquifer, chosen as one of the pilot study cases within the GEF-funded UNEP/MAP MedPartnership actions (UNEP, 2010) intended to promote the protection of the marine and coastal environment of the Mediterranean Basin.

Within this framework this paper aims at (i) presenting new hydrochemical results confirming the previous findings on aquifer dynamics, (ii) tracking the changes in groundwater composition related to the use of irrigation water from different sources, (iii) highlighting seasonal variations and impacted areas as a tool to assess the aquifer vulnerability, and (iv) fostering the protection of the Mediterranean Basin presenting a replicable example of multi-tracer approach for the support of groundwater management in rural coastal areas.

The understanding of aquifers dynamics and their relation to agricultural practices is an asset for ensuring long term management strategies for the protection of scarce water resources and ensuring food security in arid and semiarid zones. Therefore results are used to evaluate the sustainability of current agricultural practices and to propose guidelines for promoting improved water management in the Mediterranean rim countries.

2. Site description

The Bou-Areg coastal plain is located in the Mediterranean shore of Morocco, in the region of Nador (Fig. 1), and is considered one of the most important irrigated areas in North-Eastern

Morocco. The alluvial plain of Bou-Areg covers a surface area of about 190 km^2 and it is limited by the Gourougou volcanic massif (NW), the Beni-Bou-Iffrour Massif and the Kebdana range (SE); its northern boundary coincides with the arched shape of the Lagoon of Nador (also known as Marchica or Sebkha Bou-Areg), while to the south the plain is connected to the adjacent Gareb plain through the Selouane corridor (El Amrani et al., 2005). The Gareb plain is a basin oriented WSW-ENE, separated from the Bou-Areg plain (NE) by the Plio-Villafranchian plateux located in the Selouane area, which overlays the volcanic formations of Beni Bou Ifrour (Dakki, 2003).

The Bou-Areg unconfined aquifer is comprises late-Pliocene to early Quaternary continental sediments of variable thickness (up to about 100 m) and high permeability (up to 7 x 10^{-4} m s^{-1}), limited to the bottom by a Pliocene substratum of gypsiferous marls (Chaouni Alia et al., 1997)

Its natural recharge is given by groundwater from the adjacent Gareb aquifer, rainwater, stream water from the Selouane River and runoff coming from the massifs bordering the plain. Urban and industrial wastewaters, together with irrigation returns, also contribute to the recharge. Hydraulic head in the aquifer decreases from the bordering ranges towards the Lagoon of Nador (e.g. from 40 m a.s.l. close to the Kebdana range to sea level near the shore), and represents the natural outflow from the aquifer system (Dakki, 2003).

The hydrologic network of the area is characterized by the presence of several rivers -locally named *oueds*-, some of which are ephemeral and often serve as sewage outflow for urban areas upstream (Gonzalez et al., 2007). Only few streams are perennial, the most important being the Oued Selouane (or Selouane River).

The region of Nador, as with many other coastal plains along the Mediterranean, is characterized by intense agricultural activities corresponding to more than 62% of the total surface area (El Yaouti et al., 2008; FAO, 2012), with only 20-40% constituting equipped irrigation land (FAO, 2012).

Due to the irregular precipitations and the different kinds of agricultural activities, irrigation water in the past was provided by groundwater withdrawn from hand-dug wells and boreholes. The high natural salinity of this water, its increase in the years, and the emerging soil fertility problems fostered in the 1970’s the construction on an irrigation network, whose main channel represents the border of the irrigated area (Fig. 1). Freshwater coming from the Moulouya river is stored in the Mohammed V dam (built in 1967), sent to the Mechraa-Hammadi dam (built in 1956 at the Moulouya gorge, on the western edge of Beni Snassene), diverted towards the cultivated areas through the Zebra channel and distributed via a network of minor superficial channels (Dakki, 2003). Diverted waters have been increasingly used to support agricultural activities through flood irrigation, resulting in a slow decrease of groundwater salinity over the years (El Amrani et al., 2005).

The climate of the region is semi-arid with two distinct seasons: the warm period, generally from May to October (average temperature of 23-24°C), and the cold season from November to April, (average temperatures of 15°C; data available from WeatherSpark, 2014). Seasonal climatic variations are usually moderate, with a general high level of humidity (50-80%) due to the proximity to the sea. Yearly average (1984-2014) precipitations range from 300 to 400 mm/y, and these are generally more abundant in January-March and October-December (Fig. 2). The driest months are May, June and July, with scarce or no rain episodes and higher mean temperatures, inducing a water deficit. Mean rainfall data at the Melilla-Nador station is 487 mm, and annual potential evapotranspiration, estimated using the Thornthwaite equation, rises up to 1030 mm. Total rainfall in 2010, when the field survey was conveyed, was of 482 mm in the area. Therefore, considering the timing of recharge from precipitation and irrigation, it is possible to define two periods (El Yaouti et al., 2008): (i) recharge from precipitation and low use of groundwater/irrigation channel water from October to April (L-IR) and (ii) no recharge from precipitation and high water irrigation from wells and the irrigation network from May to October (H-IR) (Fig. 2).

As previously mentioned, agriculture is the dominant sector in the region of Nador, and in particular in the Plain of Bou-Areg with more than 100 km^2 (10180 ha) of irrigated land (Agence Urbaine de Nador, 2013), exploited for both local consumption and for agro-industrial production (Khattabi and El Ghazi, 2008). The main crops include cereals, olive, citrus fruit, grapes, sugar beet, vegetables (with and without greenhouses). Another relevant sector is cattle husbandry, with sheep and goats representing the main livestock, although dairy and poultry farming is also practiced in irrigated area (Boelee and Laamrani, 2003).

Figure 1.

Figure 2.

3. Methods

Two sampling campaigns performed in June 2010 (Re, 2011) and November 2010 (Fig. 3) allowed for the collection of a total of 61 samples: 56 groundwater samples from private hand-dug wells and boreholes (< 30 m deep, Tab. X1) in the Bou-Areg aquifer and 1 in the adjacent Gareb Plain; 3 samples in the Selouane River (Oued Selouane) and 1 sample from the irrigation channel.

Sampling was carried out in the previously defined H-IR and L-IR periods in order to assess seasonal effects and the impacts of irrigation activities. Moreover, H-IR samples have been selected focusing in the agricultural zone whereas in L-IR the sampling network covered the whole plain in order to facilitate the end-member identification.

Figure 3.

In situ measurements of electrical conductivity, pH and water temperature were performed during both campaigns, using a WTW 340i multimeter. Total alkalinity was also determined in the field by titration using an HACH alkalinity test kit (Tab X1).

Samples for major ion analysis were filtered through 0.45 μm cellulose membrane and stored in high density polyethylene bottles. Samples for cation analyses were preserved by addition of 5N HNO_3 immediately after filtration. Samples for stable isotope analysis were collected and preserved according to the procedures indicated by Clark and Fritz (1997).

Chemical analyses of water samples were performed at the Department of Earth and Environmental Sciences of the University of Pavia (Italy), using a Dionex DX 120 ion chromatograph. The error, based on the charge balance, was calculated to be <5%. Hydrogen isotope compositions (δ^2H) were measured by water reduction over metallic zinc (Coleman et al., 1982), while oxygen isotopes ($\delta^{18}O$) were analyzed by water-CO_2 equilibration at 25 °C (Epstein and Mayeda, 1953). Both results are expressed in ‰ vs Vienna Standard Mean Ocean Water (V-SMOW; Gonfiantini, 1978; Gonfiantini et al., 1995) with uncertainties (2σ) of ±1‰ and ±0.1‰ respectively. The $\delta^{13}C$ of DIC was analyzed by direct acidification of the water sample with phosphoric acid (Kroopnick, 1974). Results are expressed in ‰ vs Vienna Pee Dee Belemnite (V-PDB; Gonfiantini, 1978; Gonfiantini et al., 1995), and the uncertainty (2σ) is ±0.3‰. $\delta^{15}N_{NO3}$ and $\delta^{18}O_{NO3}$ of dissolved nitrate were analyzed following the procedures described by Silva et al. (2000) and refer to AIR and V-SMOW (Gonfiantini et al., 1995) with uncertainties (2σ) of ±0.5‰ and ±1‰ respectively. All samples were prepared and analyzed on a Finningan™ MAT 250 Mass Spectrometer at ISO4 private laboratory, Turin (Italy).

Saturation indices for gypsum and carbonates and partial pressure of CO_2 (pCO_2) were calculated using PhreeqC, (Parkurst and Appelo, 1999) while total alkalinity was calculated with the software AquaChem™ (Schlumberger Water Services).

The spatial distribution of conductivity data was compiled using the kriging algorithm included in the GS Surfer® package (Golden Software, Inc., Golden, CO, USA, 2008).

Statistical data treatment, in the form of Principal Component Analysis (PCA; e.g., Chatfield and Collins, 1980) was performed using the statistical package SPSS 15.0 for Windows® (SPSS, Inc., Chicago, IL, USA, 2004).

4. Results

Samples collected in the Bou-Areg aquifer have a general high Electrical Conductivity (EC; Tab X1), ranging from 1.74 mS/cm (well 5b) to 10.52 mS/cm (well 4; average 5.971 mS/cm) in June 2010 and 1.78 mS/cm (well 5b) to 10.66 mS/cm (well 32; average; 6.08 mS/cm) in November 2010.

Conductivity maps (Fig. 4), show a similar distribution of this parameter for both sampling campaigns. Higher EC values are found in the south eastern part of the investigated area (near the lagoon shore and close to the city of Kariat Arkmane; wells 3, 4, 15, 32), but also in proximity of the Gareb Plain (wells 10, 27, 34) and in the so-called Selouane Corridor, hosting the river (e.g. wells 6b, 7b, 30, 37). These maps indicate that, despite some changes in the location of the sampled wells, both datasets are comparable and suggest the existence of multiple sources of salinity in the investigated area.

Figure 4.

Figure 5.

On the Durov diagram (Fig. 5) both campaigns can be clearly distinguished. Samples of the L-IR period display a rather constant sodium-chloride hydrochemical facies whereas the relative proportions of Na^+ and Cl^- decrease in samples of the H-IR period, resulting in a higher variability of hydrochemical facies from sodium-sulphate to sodium-bicarbonate. Such seasonal variability is not associated with dramatic changes in pH (range 7-8) or TDS (range 900-6000 mg/L; Tab. X2). Nevertheless, it is interesting to note that in the TDS part of the Durov diagram, most of the groundwater samples from the H-IR period plot on a line connecting the composition of the irrigation channel and the Selouane River from the L-IR period (red dashed line in Fig. 5) whereas those from the November campaign show also a linear trend, yet with lower Ca+Mg concentrations (in meq %) than those from June.

Finally, another feature of the studied area is the groundwater high nitrate content, with most samples having nitrate concentrations exceeding the drinking water standard of 50 mg NO_3^-/L (WHO, 2011) both in the rural and urban/peri-urban areas (Re et al., 2013b). The origin of this ion has been investigated in detail using nitrate isotopes (Re et al., 2013a) allowing to identify manure and septic effluents, especially in urban areas and in the central part of the plain, and synthetic fertilizers in the agricultural zone as the main drivers for human induced pollution.

PCA was performed on 61 observations (i.e. all the samples collected in L-IR and H-IR, including the irrigation channel and the Selouane River), considering 16 hydrochemical and isotopic variables (pH, EC, total alkalinity, HCO_3^-, pCO_2, Cl^-, NO_3^-, SO_4^{2-}, Na^+, K^+, Ca^{2+}, Mg^{2+}, $\delta^2 H$, $\delta\ ^{18}O$, $\delta\ ^{13}C$ and SI_{Gypsum}). The value of 1424.86 for the Barlett chi-square statistic (120 degrees of freedom and a minimum significance level of 0.00) applied for the Barlett's sphericity test indicates the existence of a good correlation between the variables. Moreover, the measure of sampling adequacy (MSA) obtained by the Kayser Meyer Olkin (KMO) measure returns a rather high value (0.636), validating the PCA application. In order to obtain higher values in this measure pH has been excluded from the analysis given the poor correlation with most of the variables. To reduce the overlap of the original variables over each principal component a Varimax rotation was performed (Kaiser, 1985).

PCA results are presented in Table 1, including the loadings, the eigenvalues, the amount of variance explained by each varifactor (VF) and the cumulative variance.

Table 1.

5. Discussion

The characteristic high salinity of the Bou-Areg groundwater (cfr TDS Tab. X2 and EC values in Fig. 4, using EC as a proxy for salinity) has been pointed out by several authors (Chaouni Alia et al., 1997; El Amrani et al., 2005; El Mandour et al., 2008; El Yaouti et al., 2009; Re et al., 2013a) and generally attributed to the combined action of dissolution processes of evaporites and carbonates from Miocene substratum, water-rock interactions, as well as human inputs, such as agricultural return flows (Re et al., 2013a). As previously mentioned in both H-IR and L-IR periods all groundwater samples (apart from well 5b) have EC values greater than 2500 µS/cm, hence unsuitable for irrigation (Ayers and Westcot, 1994). In addition, in order to better support and promote new integrated irrigation strategies, it is also important to understand how irrigation (and consequently, agricultural return flows) affects groundwater quality.

5.1. Influence of irrigation on groundwater quality

The different sources and processes associated with groundwater recharge are well illustrated in Fig. 6, which compares chloride and sulphate contents in H-IR and L-IR periods. In the figure groundwater compositions of the Gareb Plain (J10,) and of the Selouane River, representing the saline end-members, are clearly distinguished from the irrigation channel. All samples collected in the Bou-Areg aquifer show elevated sulphate concentrations that are attributed to the influence of marly-gypsum outcrops, especially in the upstream zone, as pointed out by El Yaouti et al. (2009). Among the samples collected in H-IR, some have concentrations consistent with the composition of the Selouane River (River Recharge-RR), suggesting a possible occurrence of local lateral recharge from the river or a greater influence of groundwater from the Gareb Plain. Other samples show lower Cl values that might be attributed to a greater impact of waters from the irrigation channel, (Agricultural Return Flow-ARF) as proven by the composition of well J5b , the closest to the irrigation channel (Fig. 3; Cl^-: 150 mg/L; SO_4^{2-}: 385 mg/L; irrigation channel; Cl^-: 125 mg/L; SO_4^{2-}: 365 mg/L). These results indicate the occurrence of a dilution effect of irrigation waters infiltrating in the central part of the aquifer on the general high natural groundwater salinity (El Yaouti et al, 2009; Re et al., 2013a). Only few wells (mainly in L-IR) show intermediate concentrations with respect to the previously described groups. For those wells, salinity content originates from a mixing of irrigation and river recharge or by further dissolution of rock bearing minerals during infiltration of irrigation return, leading to a "natural water-rock interaction" hydrochemical facies (Mixing-MIX).

A different scenario can be deduced from the November 2010 samples (Water-Rock Interaction-WRI; Fig. 6), when the impact of irrigation activities is lower. Here none of the samples showed a composition consistent with that of the irrigation channel, and even well 5b shifts its November composition towards a decrease of SO_4^{2-} and an increase in Cl^-, tending to the natural high salinity of the aquifer.

Therefore, the groundwater hydrochemical composition in the two periods reflects the impact of the irrigation practices. In fact, recharge from high precipitation and low water irrigation from the channel occurs from November to April (El Yaouti et al., 2008) while a period of low precipitation recharge and high water irrigation from both the canal and groundwater takes place from May to October. Hence we can assume that in L-IR period the system is less affected by human induced recharge and, therefore, it shows a more natural composition, due to dominant water-rock interaction processes.

Figure 6.

Based on the features evidenced by the SO_4^{2-} versus Cl^- plot, groundwater samples have been attributed to the previously described groups. For such groups, means and standard deviations of each parameter in the different seasons are presented in Tab. X3.

While sulphates and chloride are indicative of water-rock interaction processes, carbonate equilibria are highly reactive and can be used in conjunction with $\delta^{13}C$ of DIC to highlight biological processes influencing groundwater chemistry. As already shown by the Durov diagram (Fig. 5), a major difference in groundwater chemistry between H-IR and L-IR periods is related to the bicarbonate content, which is sensibly higher in the former (Fig. 7A). This higher content is not strictly related to an increase in groundwater pH, but rather to a higher pCO_2 (Fig. 7B), likely attributable to a more intense biological activity in irrigated soils during the May-October period. Indeed, most of the samples from the November campaign, and those from the Oued Selouane, lay on the pH-pCO_2 line corresponding to calcite saturation under open system conditions, whereas samples from the June survey show a slight displacement towards higher pH values for similar initial pCO_2 conditions, which indicates a tendency towards closed system conditions in the system H_2O-CO_2-$CaCO_3$ (Drever, 1982).

Saturation indices for carbonates and gypsum are plotted with respect to TDS in Fig. 7C and 7D respectively. It appears that, while groundwater samples from the L-IR period are generally undersaturated with respect to carbonates, they become oversaturated during the H-IR period. The same observation does not apply to gypsum saturation, which instead only depends on the groundwater TDS.

Additional information can also be obtained from $\delta^{13}C$ measurements in DIC (Fig. 7E), especially when the behavior the carbonate system between the two periods is compared (Fig. 7F). Several processes, all associated with agricultural practices, could potentially be responsible for changes in Ca^{2+} content, as indicator of calcite weathering, and $\delta^{13}C$:

1) an increase in the soil biological activity, increasing the soil pCO_2 which is buffered in the subsurface by carbonate dissolution from the aquifer matrix. In this case, we should expect high Ca^{2+} concentrations in the H-IR period, as well as high $\delta^{13}C$ values (assuming soil carbonates have a dominant marine signature);
2) an increase in the soil biological activity influencing the soil pCO_2 whereas irrigation water dissolves gypsum precipitated in the unsaturated zone. In this case, Ca contents should increase with no appreciable change in $\delta\ ^{13}C$ values;
3) a direct influence of the isotopic composition of rechargewater

In Fig. 7E, a remarkable feature of groundwater samples from the L-IR period is that the previously defined groups are characterized by distinctive Ca concentrations at varying pCO_2, yet in agreement with their water origin and hydrogeological evolution. However, in the H-IR period, WRI, MIX and ARF groups display an increase in Ca^{2+}, at higher pCO_2, likely resulting from the intense root activity during the crop growing season. Regarding $\delta^{13}C$ a large range of values was observed in both sampling periods, from $\delta^{13}C \approx -14.0‰$ to -5‰. However, the main recharge sources (i. e, the Oued Selouane and the irrigation channel), have enriched $\delta^{13}C$ contents (-6‰ and -9‰, respectively) which are in agreement with those groundwater samples attributed to river recharge (RR). Nevertheless, those samples whose origin is related to water-rock interactions (WRI) and agricultural return flow (ARF) generally show lower $\delta^{13}C$ contents which are consistent with a higher contribution of soil carbon dioxide of organic origin that dissolves calcite in its path towards the water table, even during the L-IR, when pCO_2 and infiltration rate are small. In summary, $\delta^{13}C$ values confirm the different sources and processes occurring at the Bou-Areg aquifer that were previously identified using hydrochemical data.

Furthermore, specific L-IR samples as those with $\delta^{13}C < -11‰$ that show a decreasing trend on the plot of pCO2 (Fig. 7F) and low SI_{cal} (Fig. 7C), belong to wells influenced by urban impacts. Indeed, although the majority of the households (~47%) are connected to the sewage network, septic tanks are still widely used (~ 29% of the households) for wastewater evacuation in both the rural and peri-urban area (Khattabi and El Ghazi, 2008), still representing one of the main drivers for groundwater contamination.

It must also be considered that cation exchange in the aquifer may be responsible for a decrease in Ca^{2+} and an enrichment in Na^+ content in groundwater (El Yaouti, 2009). This additional process may explain some low SI_{cal} values during the November campaign (when the infiltration rate of rainfall is assumed smaller than that of the irrigation period), and some general gypsum undersaturation.

Figure 7.

Figure 8.

Isotopic data (δ^2H and δ^{18}O) also show different behaviors between the June and November campaigns. In fact, considering the isotopic composition of the water molecule (Fig. 8) with respect to the Global Meteoric Water Line (GMWL, Rozanski et al., 1993) all the samples appear to be enriched in oxygen-18, suggesting the occurrence of evaporation processes, as already indicated by Re et al. (2013a). Indeed, samples from both campaigns may be distributed along two evaporation trend lines (namely, EVAP-1 and EVAP-2, in Fig. 8), with slopes around 5.2, which correspond to evaporation with an environmental humidity of 75% (Gonfiantini, 1986); this value is in agreement with the mean annual atmospheric humidity in the Nador Airport weather station (WeatherSpark, 2014).

In the L-IR period, when, based on hydrochemical data, groundwater compositions are mostly determined by natural water-rock interaction processes, the regression line (δ^2H = 5.34 δ^{18}O - 6.60; R^2= 0.77; n= 26, i.e. excluding N31 which is out of the Bou-Areg basin) crosses the GMWL at a value of about -5.9‰ in δ^{18}O and – 38‰ in δ^2H. This value could be attributed to the mean rainfall isotopic composition in the Nador area, although no measured data are available, as it is roughly in agreement with the interpolated precipitation compositions for the region (Bowen and Revenaugh, 2003). This finding suggests that during the L-IR period groundwater is mostly recharged by local precipitation affected by evaporation prior to infiltration (line EVAP-1 in Fig. 8). According to Gonfiantini's equations, the largest evaporation percentage would be less than 5%, indicating a short ponding time in the field surface or evaporation in the vadose zone (Gonfiantini, 1986). In the H-IR period, the more depleted values correspond to the irrigation channel and well J5b, the closest to the irrigation channel. Assuming the isotopic composition of irrigation water as an end-member, a similar evaporation process could account for the isotopic composition of most groundwater samples (EVAP-2) influenced by irrigation water. The lines EVAP-2 and GMWL cross at an isotopic value of about -7‰ in δ^{18}O and – 47‰ in δ^2H. Such depleted values for meteoric waters may correspond to precipitation at higher altitudes in the Atlas chain, and they are seldom recorded in the south-western Mediterranean coast (Saighi, 2005). Indeed, such hypothetical values are in good agreement with the isotopic composition of the Moulouya river feeding the Mohammed V basin (-6.92‰ in δ^{18}O and – 47.7‰ in δ^2H; inverted triangle figure Fig. 8; IAEA, 2010.), where water is stored and likely evaporated prior to being diverted to the Zebra irrigation channel. The irrigation channel sample shows an evaporation percentage of ≈5%, based on isotopic data, and subsequent evaporation after irrigation increases it up to a 7.5% (Gonfiantini, 1986). As already evidenced by hydrochemical parameters, and also supported by isotopic data, mixing with seawater is not occurring in the Bou-Areg aquifer, except in a few wells nearby the Nador Lagoon. Therefore, the prevailing mechanism for groundwater salinization is the dissolution of salt minerals and agricultural as well as urban inputs to the subsurface.

5.2 Statistical data treatment

PCA was performed in this study to better support geochemical evidences, identify end-members, and understand the seasonal variability and its relation with agricultural activities (Menció et al. 2012). Three varifactors were extracted (Table 1) with a total cumulative variance explained of about 75%. In particular, each varifactor provides the following hydrogeological associations:

- Varifactor 1 (VF1) explains 41.3% of the total variance and is participated by EC, Ca^{2+}, Cl^-, SI_{Gypsum}, Na^+, Mg^{2+}, SO_4^{2-}, and $\delta^{13}C$. This varifactor is thus representative of the total aquifer salinization, including both mixing processes and lateral river recharge (Fig. 9A). For both the campaigns, the samples with positive scores (VF1>0) belong to RR or MIX groups, while lower scores (VF1<0) characterize the samples where agricultural return flow and water rock interaction processes dominate.
  Hence, high values of V1 imply high aquifer salinization, but do not allow for a clear distinction between L-IR and H-IR (as VF1 also includes K^+, Ca^{2+} and SO_4^{2-}).
- Varifactor 2 (VF2), with 21.9% of the variance, is highly correlated with HCO_3^-, total alkalinity and pCO_2, and refers to carbonate equilibria. HCO_3^- increase (and positive relation with VF2) for H-IR samples (Fig. 9B) was previously explained by their high bicarbonate content being determined by the increased biological activity (i.e., higher pCO_2) during the crop growing season. In addition, the negative correlation between VF2 and δ^2H (Table 1) suggests that high irrigation activities correspond to samples with lower δ^2H, with the lowest values associated with the irrigation channel. VF2, related to δ^2H also distinguished those samples along the evaporation lines EVAP1 and EVAP2, which indeed relates to the water origin in the area. This reinforces the role of the irrigation channel water for aquifer recharge, especially during H-IR.
- Varifactor 3 (VF3), explaining 12.2% of the variance, includes $\delta^{18}O$ (highest weight), δ^2H, NO_3^-, and it is negatively correlated with $\delta^{13}C$. This varifactor corresponds to the nitrate pollution trend (Fig.9C). In fact, an increase in VF3 is associated with an increase in $[NO_3^-]$, in most of the cases due to agricultural pollution in H-IR. By comparison, most of the samples of the L-IR period, with lower NO_3^- contents, generally display negative scores for VF3. The positive correlation of VF3 with $\delta^{18}O$ and δ^2H indicate that nitrate content is larger in isotopically enriched samples corresponding to low altitude recharge (Menció et al., 2011). L-IR samples with a larger VF3 score are located in the urban/peri-urban area of Nador (N8b, N36, N38 and N39) and reflect the strong contribution of domestic pollution, as pointed out by Re et al. (2013b). Only for sample N33, located in the rural zone and having the highest $\delta^{18}O$ value for the L-IR campaign but low nitrate contents, the large VF3 score is likely related to the higher contribution of $\delta^{18}O$ in VF3. On the other hand samples J1, N7 and N28 (Fig.9C) are also likely to be affected by local (point source) contamination (i.e. manure and/or septic effluents) in the agricultural part of the Bou-Areg Plain.

Figure 9.

Fig. 10 shows the correlation between the main varifactor scores for each sample. In the plot of VF1 (salinization) versus VF2 (soil biological activity; Fig. 10A), samples are consistently grouped with the groups identified by the geochemical interpretation. In particular, VF2 clearly distinguishes L-IR from H-IR samples. The dominant driver for groundwater composition in H-IR is the increasing soil biological activity during the crop growing season, as also detected by comparing VF2 and VF3 (Fig. 10C). Concerning those samples under the influence of the Selouane River recharge (RR), they appear to be dominated by different factors, according to the season: in L-IR, groundwater composition is mainly influenced by a recharge from the Selouane River (plotting in the second quadrant, Fig.10A), while in H-IR groundwater samples are also affected by biological activity (orange samples in the first quadrant, Fig. 10A), as indicated by a low, yet positive, score of VF2. On the other hand no relationship between VF1 and VF2 is visible for WRI samples and the irrigation channel (third quadrant Fig 10A), highlighting the relatively low salinization due to the absence of irrigation activities.

In the VF1 (salinization) versus VF3 (nitrate pollution) plot, different situations can be described. Some samples are characterized by high values of VF3 (fourth quadrant, Fig.10B), highlighting the occurrence of agricultural pollution (ARF) and contamination from manure and septic tanks in the urban area (see also Fig. 10C). In the second quadrant (high scores in VF1 and low scores in VF3) plot the RR and some of the MIX samples, which are characterized by high salinization rather than nitrate pollution, whereas neither salinization nor nitrate pollution affects the composition of the irrigation channel waters and the L-IR samples in the agricultural zone (Fig. 10B). In other words, samples in quadrants I and IV are those related to urban pollution or groundwater use for irrigation (local recharge - given the high contribution of δ^2H, $\delta^{18}O$ in VF3 - and high nitrate pollution). Samples with the lowest NO_3^- pollution and river influence lay in quadrant II, while those samples with highest channel influence, lower $[NO_3^-]$ (in H-IR), and the aquifer signature characteristics (L-IR) are located in quadrant III.

PCA analysis synthesize the fact that samples can be distinguished by soil biological activity magnitude, as HCO_3^-, pCO_2 and $\delta^{13}C$ contents, while they may be affected by a wide range of salinization and nitrate pollution levels, depending on land use and on anthropogenic pressure on water resources. The two main groundwater recharge sources, the irrigation channel and the Selouane River, consistently relate to the samples scores, supporting the hydrogeochemical conclusions reached in the previous discussion.

Figure 10.

5.3 Water management issues

When groundwater resources, such as those found in the Bou-Areg aquifer, are used for irrigation, their high salinity content can eventually accumulate in the crop root zone and cause yield reduction (Ayers and Westcot, 1994). As a result, the crop is no longer able to extract sufficient water from the salty soil solution, resulting in a water stress for a significant period of time. Good quality irrigation water is therefore essential for ensuring crop productivity, and water salinity is thus a serious limiting factor, especially for crops with limited salt tolerance (fruits, citrus, beans). Although since the construction of the irrigation channel groundwater withdrawal for this purpose significantly decreased, farmers with equipped wells still resort to –costless- groundwater, neglecting its negative effect on crop productivity.

Besides the ascertained salinity of the aquifer and its impact on agricultural activities, it is also important to define how irrigation (and agricultural return flows) affects the natural groundwater quality and quantity, in order to better support and promote new integrated irrigation strategies. Moreover, excluding groundwater, the Moulouya River resources, which feed the irrigation channel in the study area, represent almost 90% of the water used for irrigation in all the North-Eastern coastal plains of Morocco (Sebra, Bou-Areg and Gareb plains). However, its runoff is severely threatened by the combined impact of climate change and silting of the Mohammed V dam, where water is stored prior to distribution (Dakki, 2003). In addition, the rapid demographic increase and growing tourist sector (for instance, the new MarchicaMed project, along the sand bar that limits the Nador lagoon with the open sea) will also compete for water resources allocation, and will contribute to the decrease in water available for irrigation. A lack of adequate planning taking into account the hydrodynamics of the hydrogeological system may represent a further, irreversible impact to the area, as already observed in many locations, especially along the Mediterranean coast.

In summary, some specific issues arise from the Bou-Areg aquifer study that may lead to further improvements in water resources management in the region, as well as being replicated in similar contexts along the Mediterranean shore:

- Despite a high vulnerability to agricultural (and urban) pollution the Bou-Areg coastal aquifer has shown a good resilience to intense agricultural activities as proven by the seasonal hydrochemical variations.
- Channel water from the Moulouya River has the best quality with the lowest EC values and the lowest [NO_3^-]. Therefore this resource must be protected from contamination and excessive exploitation in its headwaters, in order to allow irrigation in the lowlands. Further agricultural and tourist development should face water scarcity (present and future) to ensure smart water allocation that fosters economical as well as social development and environmental preservation.

- Selouane River presents the highest EC values and medium [NO_3^-], hence groundwater withdrawal close to this river, possibly causing head level decrease, can lead to stream leakage to the aquifer and thus, aquifer salinization. Extended irrigation of the area using channel water may lead to a decrease the infiltrating rate of stream water, thus enhancing groundwater quality and allowing a larger discharge for surface dilution processes and ecosystem services.
- The highest [NO_3^-], concentrations have been mainly attributed either to urban or to agricultural sources. Previous studies (Re et al., 2013a; Re et al., 2013b) pointed out that septic effluent (especially in urban areas), agricultural return flow, or a mixing of these processes, are responsible for such high concentrations. This implies that improved sanitation facilities and a better control on groundwater withdrawal and fertilizer use are of paramount importance for both water quality protection and food security issues.
- Finally, the increasing climatic uncertainty coupled with the potential emerging conflicts in water use (agriculture, tourist and industrial sector) will probably put water scarcity issues at the highest level of planning and management discussions. Alternative irrigation sources, such as reclaimed wastewater reuse, may be of capital relevance. Moreover, the available hydrochemical information relates only to the upper levels of the Bou-Areg aquifer system. Research on groundwater quality in deeper layers may evidence alternative water resources (e.g. large scale flows system, paleowaters) whose sustainable exploitation should be carefully evaluated.

Figure 11.

6. Conclusions

In the framework of a common strategy for the safeguarding and long-term protection of the Mediterranean coastal zones, this study presents a hydrogeochemical characterization of aquifer dynamics and pollution of the Bou-Areg aquifer, identified as one of the pollution hot-spots under investigation in the MedPartnership actions.

Results of the hydrogeochemical and multivariate analysis of the Bou-Areg aquifer on samples collected in 2010 show a strong seasonal variation of groundwater quality, mainly associated with the impact of agricultural practices. In absence of irrigation activities (L-IR), natural water-rock interaction processes and pollution inputs from civil sources control the salinity of the system, together with a possible contribution of groundwater from the nearby Gareb Plain through the Selouane corridor. On the other hand, during the irrigation season (H-IR) the impact of irrigation practices is associated with an increase of the soil biological activity and of agricultural pollution, mainly consisting of high nitrate concentrations in groundwater.

The coupled hydrogeochemical and multivariate analysis proved to be a useful tool for the clear identification of following dominant processes governing the aquifer's hydrochemistry in the different seasons: (Fig. 11):

- Water Rock Interaction processes (WRI) dominate the composition of most of groundwater samples in L-IR. In some cases, especially in the peri-urban area of Nador (left bank of the Selouane River) human activities also affect the natural composition of the aquifer, resulting in severe nitrate contamination (Re et al., 2013a);
- Agricultural Return Flow (ARF) mainly affects groundwater salinization in H-IR in the same areas naturally affected by WRI. However, a strong seasonality effect governs groundwater quality in the aquifer,
- River Recharge (RR) is responsible for the high salinity of the samples in the proximity of the Selouane River. This can be associated with natural lateral discharge or to stream capture driven by groundwater abstraction in the irrigation season. Groundwater flow from the Gareb Plain may contribute to the background hydrochemical composition of the aquifer.
- Mixing Processes (MIX) occur along the Selouane corridor, in absence of irrigation activities. Here, groundwater chemical composition is influenced both by the Selouane River, or groundwater coming from the Gareb Plain, and WRI processes.

As discussed, these findings have sound management implications and must be taken into account for future agricultural development plans of the region. In fact, the high aquifer vulnerability implies the need to better control both the quantity and the quality of irrigation waters. Managing the impacts of agricultural return flow and urban inputs will enhance groundwater quality with relevant positive effects on crop efficiency, soil salinization, and environmental issues. Conversely, results highlight the need for a more efficient use of available water resources coupled with the identification of alternative irrigation sources, and the implementation of more efficient agricultural practices.

Acknowledgements

This study was partially supported by the Italian Ministry for Environment, Land and Sea as a contribution to the GEF UNEP/MAP Strategic Partnership for Mediterranean Sea Large Marine Ecosystem (MedPartnership) under the sub-component executed by UNESCO-IHP on the ‘‘Management of Coastal Aquifer and Groundwater’’. The authors would like to thank Prof. N. El Hamouti and Mr. R. Bouchnan for the help during the June 2010 sampling campaign, and Dr. T. Lovato for his support during the November 2010 one. We are grateful to UNESCO-IHP and UNESCO office in Rabat (Morocco) for the technical support during the execution of the project. We thank Dr. Enrico Allais and ISO4, for their help in the chemical and isotope analysis.
In loving memory of Prof. G.M. Zuppi, coordinator of the project.

References

Agence Urbaine de Nador, 2013. http://www.aunador.ma/def.asp?codelangue=23&id_info=1467 (consulted online July 2013).

Ayers, R.S. and Westcot, D.W. 1994. Water quality for agriculture. FAO Irrigation and Drainage Paper 29 Rev.1, Roma, 174 p

Boelee, E, and Laamrani H., 2003. Multiple use of irrigation water in Northern Morocco. In: proceedings of the International Symposium on Water, Poverty and Productive uses of Water at the Household Level. 21-23 January 2003, Muldersdrift, South Africa. 35-43.

Boulabeiz, M., 2011. Évaluation du risque des eaux souterraines à la pollution : Cas de la nappe de Collo, Nord-Est Algérie. Congrès GeoHydro (Eau et Terre: la jonction des géosciences du Quaternaire et de l'hydrogéologie), Québec, Canada.

Boy-Roura, M., Nolan B.T. Menció A., Mas-Pla J. 2013. Regression model for aquifer vulnerability assessment of nitrate pollution in the Osona region (NE Spain). Journal of Hydrology, 505:150-162.

Bowen, G.J. and Revenaugh, J. 2003. Interpolating the isotopic composition of modern meteoric precipitation. Water Resources Research, 39, 1299.

CantylMedia, 2014. http://www.weatherbase.com/weather/weather.php3?s=83306&units=metric (Consulted online, June 2014)

Chaouni Alia, N., Halimi, N. El., Walraevens, K., Beeuwsaert, E., De Breuck, W., 1997. Investigation de la salinization de la plaine de Bou-Areg (Maroc nord-oriental). Proceedings and Reports of the International Association of Hydrological Sciences, Freshwater Contamination. 243, 211-220.

Chatfield, C., Collins, A.J. 1980. Introduction to Multivariate Analysis. Chapman and Hall, London, pp. 256.

Clark, I., and Fritz,P. 1997. Environmental Isotopes in Hydrogeology, Chapter 10. CRC Press. pp. 328.

Coleman, M.L., Sheppard, T.J., Durham, J.J., Rouse J.E., Moore, G.R. 1982. Reduction of water with zinc for hydrogen isotope analysis. Anal. Chem. 54, 993-995.

Croon F.W., 2013. Practical aspects of irrigation of biosaline crops with saline water viewed from a land and water use perspective. Irrigation and Drainage. DOI: 10.1002/ird.1786.

Dakki, M., 2003. Diagnostic pour l'aménagement des zones humides du Nord-Est du Maroc: 2. Sebkha Bou Areg (lagune de Nador). MedWetCoast Project, Final Report, p 54.

Drever, J.I., 1982. The Geochemistry of Natural Waters. Prentice-Hall Inc., pp. 388.

El Amrani, N., Benavente, J., El Mabrouki, K., Hidalgo, M.C., Larabi, A., 2005. Origine de la salinité des eaux au niveau de la plaine de Bou-Areg (Nador,Maroc). Bulletin du GFHN: Milieux poreux et transferts hydriques. 51, 85-90.

El Amrani, N., Larocque, M., Banton, O., Benavente, J. 2007. Simulation de la contamination des eaux souterraines du delta du rio Adra et eutrophisation des Albuferas (Almérie-Espagne). Revue des Sciences de l'Eau 20(1):15-25. INRS, Québec (Canada).

El Yaouti, F., El Mandour, A., Khattach, D., Kaufmann, O., 2008. Modelling groundwater flow and advective contaminant transport in the Bou-Areg unconfined aquifer (NE Morocco). Journal of Hydro-Environment Research. 2, 192-209.

El Yaouti, F., El Mandour, A., Khattach, D., Benavente, J., Kaufmann, O. 2009. Salinization processes in the unconfined aquifer of Bou-Areg (NE Morocco): A geostatistical, geochemical, and tomographic study. Appl. Geochem. 24(1), 16-31.

El Mandour A., El Yaouti F., Fakir Y., Zarhloule Y., Benavente Y., 2008. Evolution of groundwater salinity in the unconfined aquifer of Bou-Areg, Northeastern Mediterranean coast. Morocco. Env. Geol. 54, 491-503.

EMWIS, 2013. http://www.emwis.net/thematicdirs/news/2012/04/morocco-aids-drought-stricken-farmers (consulted online February 2013).

Epstein, S., Mayeda, T.K. 1953. Variation of O18 content of waters from natural sources. Geochim. Cosmochim. Ac. 4, 213-224.

Food and Agriculture Organization, 2012. AQUASTAT, Global Map of Irrigation Areas – Morocco. http://www.fao.org/nr/water/aquastat/irrigationmap/index30.stm (consulted online February 2012).

Food and Agriculture Organization, 1994. Water quality for agriculture. ISBN 92-5-102263-1

Foster, S. and Ait-Kadi, M., 2012. Integrated Water Resources Management (IWRM): How does groundwater fit in? Hydrogeology Journal. 20, 415-418.

Gonfiantini, R. 1986. Environmental isotopes in lake studies. In: P. Fritz and J.C. Fontes (Eds), Handbook of Environmental Isotope Geochemistry, 2. Elsevier Scientific, pp. 113-167.

Gonfiantini, R. 1978. Standards for stable isotope measurements in natural compounds. Nature 27. 534-536.

Gonfiantini, R., Stichler, W., Rozanski, K. 1995. Standards and Intercomparison Materials Distributed by International Atomic Energy Agency for Stable Isotope Measurements: Reference and intercomparison materials for stable isotopes of light elements. Proceedings of a consultants meeting held in Vienna, December 1993, IAEA Technical Document 825.

Gonzalez, I., Aguila, E., Galan, E. 2007. Partitioning, bioavailability and origin of heavy metals from the Nador Lagoon sediments (Morocco) as a basis for their management. Environ. Geol. 52, 1581-1593.

Global Water Partnership and Development Bank of Southern Africa, 2012. Regional Approaches to Food and Water Security in the Face of Climate Challenges. Proceedings, May 2011 workshop. http://www.gwp.org/Global/About%20GWP/Publications/PROCEEDINGS_Regional%20approaches%20to%20food%20and%20water%20security_final.pdf.

Global Water Partnership (GWP), 2013. http://www.gwp.org/en/gwp-in-action/Mediterranean/# (consulted online February 2013).

International Atomic Energy Agency, 2010. Atlas of isotope hydrology-Morocco. –ISBN 978-92-0-111010-7.

International Water Management Institute, 2007. Water for Food, Water for Life: A Comprehensive Assessment of Water Management in Agriculture. ed. David Molden, Earthscan, London and International Water Management Colombo.

Kaiser, H.F., 1958. The varimax criteria for analytical rotation in factor analysis. Psychometrika 23, 187-200.

Kass, A., Gavrieli, I. Yechieli., Y., Vengosh, A., Starinsky, A., 2005. The impact of freshwater and wastewater irrigation on the chemistry of shallow groundwater: a case study from the Israeli Coastal Aquifer. Journal of Hydrology 300, 314-331.

Khattabi, A., El Ghazi, S, 2008. Diagnostic socioéconomique du Littoral Méditerranéen Oriental. Projet ACCMA. Ecole Nationale Forestière d'Ingénieurs, Salé BP. 511 Tabrikt SALE, MAROC. 35pp.

Kroopnick, P. 1974. The dissolved O_2-CO_2 ^{13}C system in the eastern equatorial Pacific. Deep Sea Research. 21, 211-227.

Menció, A., Mas-Pla, J., Otero, N., Soler, A, 2011. Nitrate as a tracer of groundwater flow in a fractured multilayered aquifer. Hydrological Sciences Journal, 56, 108-122. DOI: 10.1080/02626667.2010.543086.

Menció, A., Folch, A., Mas-Pla J. 2012. Identifying key parameters to differentiate groundwater flow systems using multifactorial analysis. Journal of Hydrology, 472-473: 301-313.

Navarra A., Tubiana L. (eds) 2013. Regional Assessment of Climate Change in the Mediterranean, Volume 1: Air, Sea and Precipitation and Water. Advances in Global Change Research, Vol. 50, Springer, ISBN 978-94-007-5780-6.

Oh, N.H, Pellerin, B.A, Bachand, P.A.M, Hernes, P.J., Bachand, S.M, Ohara, N., Kavvas, M.L., Bergamaschi, B.A., Horwath, W.R., 2013. The role of irrigation runoff and winter rainfall on dissolved organic carbon loads in an agricultural watershed. Agriculture, Ecosystems & Environmen. 179, 1-10.

Parkhurst, D.L., Appelo C.A.J. 1999. User's guide to PHREEQC (version 2) – A computer program for speciation, batch-reaction, one-dimensional transport, and inverse geochemical calculations. U.S. Geological Survey Water Resources Investigations Report 99-4259, 310.

Pereira, L.S., 2004. Trends for Irrigated Agriculture in the Mediterranean Region: Coping With Water Scarcity. European Water 7/8: 47-64.

Pionke, H.B., Sharma, M.L., Hirschberg, K.J. 1990. Impact of irrigated horticulture on nitrate concentrations in groundwater. Agriculture, Ecosystems & Environment. 32, 119-132.

Qadir, M., Oster, J.D., 2004. Crop and irrigation management strategies for saline-sodic soils and waters aimed at environmentally sustainable agriculture. Science of The Total Environment, 323, 1-19.

Qin, D., Qian Y., Han L., Wang Z., Li C., Zhao Z., 2011. Assessing impact of irrigation watere on groundwater recharge and quality in arid environment usin CFCs, tritium and stable isotopes, in the Zhangye Basin, Northwest China. Journal of Hydrology, 21, 194-208.

Ravikumar, P., Somashekar, R.K., Angami, M., 2011. Hydrochemistry and evaluation of groundwater suitability for irrigation and drinking purposes in the Markandeya River basin, Belgaum District, Karnataka State, India. Environ. Monit. Assess.,173, 995-6.

Re V., 2011. Groundwater in urban coastal areas: hydrogeochemical based approach for managing the transition areas: the example of the lagoon of Nador (Morocco). PhD thesis, Ca' Foscari University of Venice.

Re, V., Sacchi, E., Martin Bordes, J.L., Aureli, A., El Hamouti, N., Bouchnan, R., Zuppi G.M., 2013a. Processes affecting groundwater quality in arid zones: the case of the Bou-Areg coastal aquifer (North Morocco). Applied Geochemistry 34, 181–198.

Re, V., Sacchi, E., Allais, E., 2013b. The use of nitrate isotopes to identify contamination sources in the Bou-Areg aquifer (Morocco). Procedia Earth and Planetary Science. 7, 729–732

Romanelli, A., Lima, M.L., Quiroz Londoño O.M., Martínez D.E., Massone, H.E., 2012. A GIS-based assessment of groundwater sustainability for irrigation purposes in flat areas of the wet Pampa plain, Argentina. Environ. Manage, 50, 490-503.

Rozanski, K., Araguás-Araguás, L., Gonfiantini, R., 1993. Isotopic patterns in modern global precipitation. Geophysical Monograph. 78, 1-36.

Saighi, O., 2005. Isotopic composition of precipitation from Algiers and Assekrem. In IAEA: Isotopic composition of precipitation in the Mediterranean Basin in relation to air circulation patterns and climate. Final report of a coordinated research project 2000–2004. IAEA-TECDOC-1453, pp. 5 - 18.

Scanlon, B.R., Reedy, R.C., Gates, J.B., Gowda P.H., 2010. Impact of agroecosystems on groundwater resources in the Central High Plains, USA. Agriculture, Ecosystems & Environment. 139, 700-713.

Silva, S.R., Kendall, C., Wilkinson, D.H., Ziegler, A.C., Chang, C.C.Y., Avanzino, R.J. 2000. A new method for collection of nitrate from fresh water and the analysis of nitrogen and oxygen isotope ratios. J. Hydrol. pagine

Stigter. T.Y., Cavalho Dill, A.M.M., Ribeiro, L., Reis, E., 2006. Impact of the shift from groundwater to surface water irrigation on aquifer dynamics and hydrochemistry in a semi-arid region in the south of Portugal. Agricultural Water Management, 85, 121-132.

Suarez, D.L,, 1989. Impact of agricultural practices on groundwater salinity. Agriculture, Ecosystems & Environment. 26, 215.227

Tadesse, N., Bairu, A., Beemalingerwara, K., Gyohannes, T., 2010. Suitability of groundwater quality for irrigation with reference to hand dug wells, Hntebet Catchment, Tigray, Northen Ethiopia., Memona Ethiopian Journal of Science, 3:31-47.

United Nations Environment Programme (UNEP), 2010. Strategic Partnership for the Mediterranean Sea Large Marine Ecosystem (MedPartnership). Inception, Report, UNEP(DEPI)/MED WG.345/3.

Watanabe, A., Kasuya, M., Tsunekawa, A., Maeda, M., Sugimoto, A., Kimura M., 2008. Spatial and seasonal variations in CH4 in groundwater used for agriculture in central Japan Agriculture, Ecosystems & Environment, 127, 207-214

World Bank, 2007. Making the most of scarcity: accountability for better water management results in the Middle East and North Africa. MENA development report, DOI: 10.1596/978-0-8213-6925-8.

World Health Organization , 2011. Guidelines for drinking-water quality, fourth edition. ISBN 978 92 4 154815 1

List of Figures

Figure 1. Location of the investigated area with details of the urban and agricultural zones.

Figure 2. Mean monthly rainfall, temperature and potential evapotranspiration using data from the Mellila-Nador meteorological station 1984 to 2014 (CantylMedia, 2014).

Figure 3. Location of the sampling sites: A) Sampling network for June 2010 (H-IR) and B) November 2010 (L-IR) campaigns.

Figure 4. Distribution map of Electrical Conductivity (mS/cm) in the Bou-Areg plain in (A) June 2010 (H-IR) and (B) November 2010 (L-IR). Well 10 (June 2010, EC=7.28 mS/cm) and well 31 (November 2010; EC= 6.67 mS/cm) are not considered in the distribution since located outside the irrigated area.

Figure 5. Durov Diagram for samples collected in June (H-IR, grey circles) and November (L-IR, black triangles) 2010 in the Bou-Areg aquifer. The red dashed line highlights the trend observed for samples in H-IR period, plotting on a line connecting the composition of the irrigation channel and the Selouane River (sampled in the L-IR period).

Figure 6. Plot of Cl^- vs. SO_4^{2-} for the samples collected in June (H-IR) and November (L-IR,) 2010 in the Bou-Areg aquifer. The arrow highlights the progressive change from groundwater composition dominated by WRI processes in L-IR towards a higher impact of ARF and RR in H-IR.

Figure 7. (A) HCO_3^- versus pH; (B) pH versus pCO_2; (C) Saturation Index of Calcite versus TDS;(D) Saturation Index of Gypsum versus TDS; (E) Calcium versus $pCO_{2;}$ (F) $\delta^{13}C$ versus pCO_2 for the samples collected in in June (H-IR) and November (L-IR) 2010 in the Bou-Areg aquifer.

Figure 8. δ^2H D and $\delta^{18}O$-variations in groundwater from the Bou-Areg coastal plain for June (H-IR,) and November (L-IR) 2010 in the Bou-Areg aquifer. Black line: Global Meteoric Water Line (GMWL: $\delta\ ^2H = 8.17\ \delta\ ^{18}O + 10.35$; Rozanski et al., 1993). EVAP-1 and EVAP-2 represent the evaporative trend for November and June 2010 respectively.

Figure 9. Relationships between varifactors (VF) and the main parameters they represent for groundwater samples collected in June (H-IR) and November (L-IR) 2010 in the Bou-Areg aquifer. (A) VF1- Salinization versus Electrical Conductivity; (B) VF2 - Soil biological activity versus HCO_3^-; (C) VF3- Nitrate pollution versus NO_3^-. The red dashed line corresponds to the WHO Drinking water standard (WHO, 2011).

Figure 10. Distribution of the Bou-Areg groundwater samples according to their scores for VF1-aquifer salinization, VF2- soil biological activity and VF3- nitrate pollution.

Figure 11. Seasonal variations in the Bou-Areg aquifer and impacts of agricultural activities in (A) H-IR (June 2010) and (B) L-IR (November 2010).

List of Tables

Table 2. Loadings of 15 variables on 4 significant varifactors (VFs). Underlined values represent relevant loadings.

Supplementary data

Table X1. Physical and chemical parameters of the waters collected in the region of Nador in June 2010 (J; Re et al., 2013) and November 2010 (N).

Table X2. Geochemical results for the waters collected in the region of Nador in June 2010 (J; Re et al., 2013) and November 2010 (N).

Table X3. Mean and standard deviation for the proposed groups of water samples collected in the region of Nador in low (L-IR) and high (H-IR) irrigation.

Table 1
Click here to download Table: Table 1.docx

Variable	VF1	VF2	VF3
EC	0.959	-0136	0.013
Ca^{2+}	0.943	0.087	-0.026
Cl^-	0.936	-0.070	-0.106
SI_{Gypsum}	0.902	0.142	0.094
Na^+	0.852	-0.298	-0.063
Mg^{2+}	0.812	0.331	0.006
SO_4^{2-}	0.777	0.023	0.123
K^+	0.611	0.081	0.227
HCO_3^-	-0.074	0.952	0.154
Total Alkalinity	-0.066	0.947	0.151
pCO_2	0.092	0.882	0.146
δ^2H	0.184	-0.645	0.588
$\delta^{18}O$	0.122	0.031	0.860
NO_3^-	-0.236	-0.150	0.601
$\delta^{13}C$	0.467	0.074	-0.474
Eigenvalues	6.201	3.283	1.831
% Variance explained	41.339	21.884	12.206
% Cumulative variance	41.339	63.223	75.430

Table 1. Loadings of 15 variables on 4 significant varifactors (VFs). Underlined values represent relevant loadings.

Figure 1

Click here to download Figure: Figure 1.docx

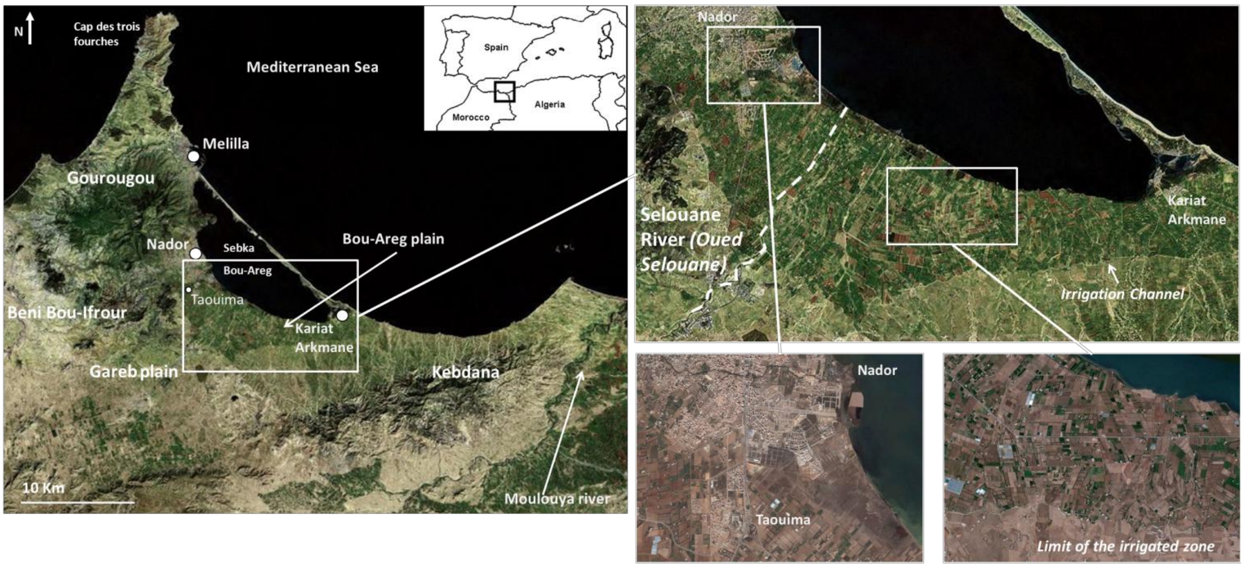

Figure 1. Location of the investigated area with details of the urban and agricultural zones.

Figure 2
Click here to download Figure: Figure 2 .docx

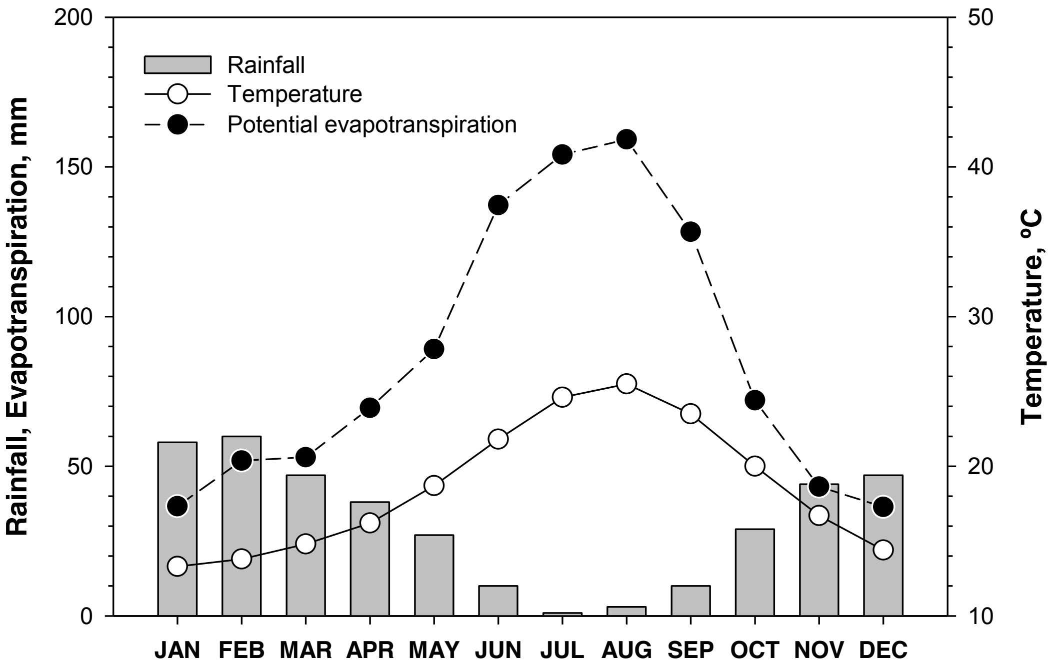

Figure 2. Mean monthly rainfall, temperature and potential evapotranspiration using data from the Mellila-Nador meteorological station 1984 to 2014 (CantylMedia, 2014).

Figure 3
Click here to download Figure: Figure 3.docx

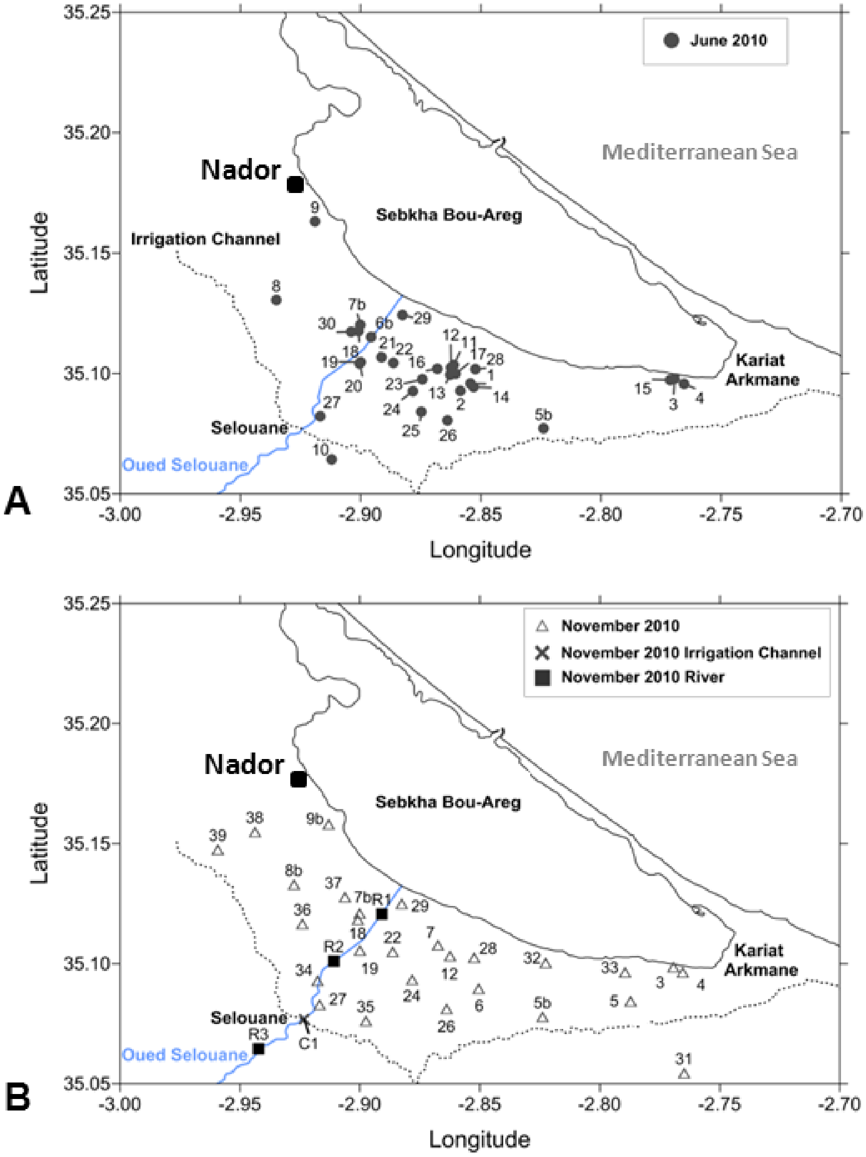

Figure 3. Location of the sampling sites: A) Sampling network for June 2010 (H-IR) and B) November 2010 (L-IR) campaigns.

Figure 4

Click here to download Figure: Figure 4.docx

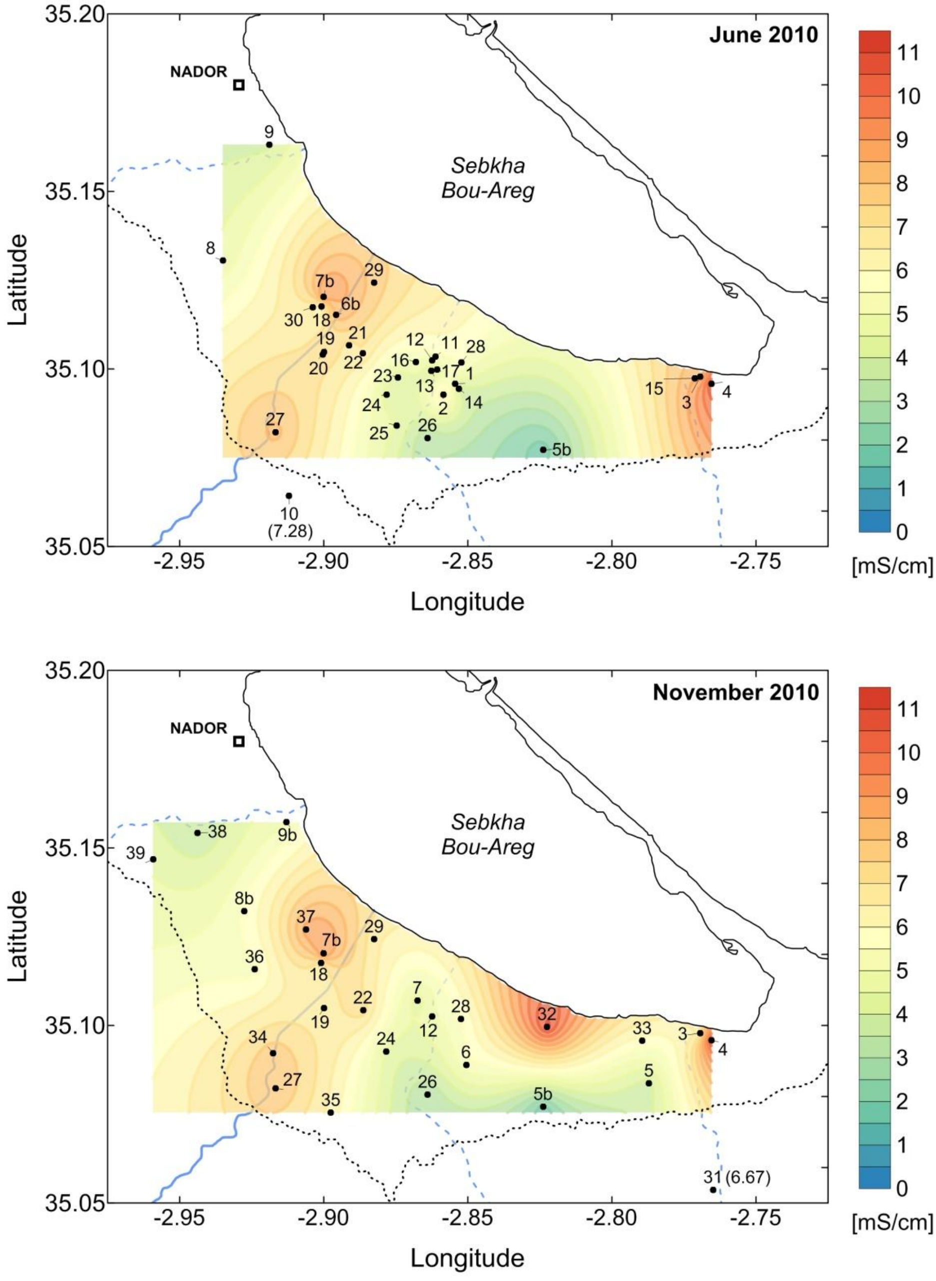

Figure 4. Distribution map of Electrical Conductivity (mS/cm) in the Bou-Areg plain in (A) June 2010 (H-IR) and (B) November 2010 (L-IR). Well 10 (June 2010, EC=7.28 mS/cm) and well 31 (November 2010; EC= 6.67 mS/cm) are not considered in the distribution since located outside the irrigated area.

Figure 5

Click here to download Figure: Figure 5.docx

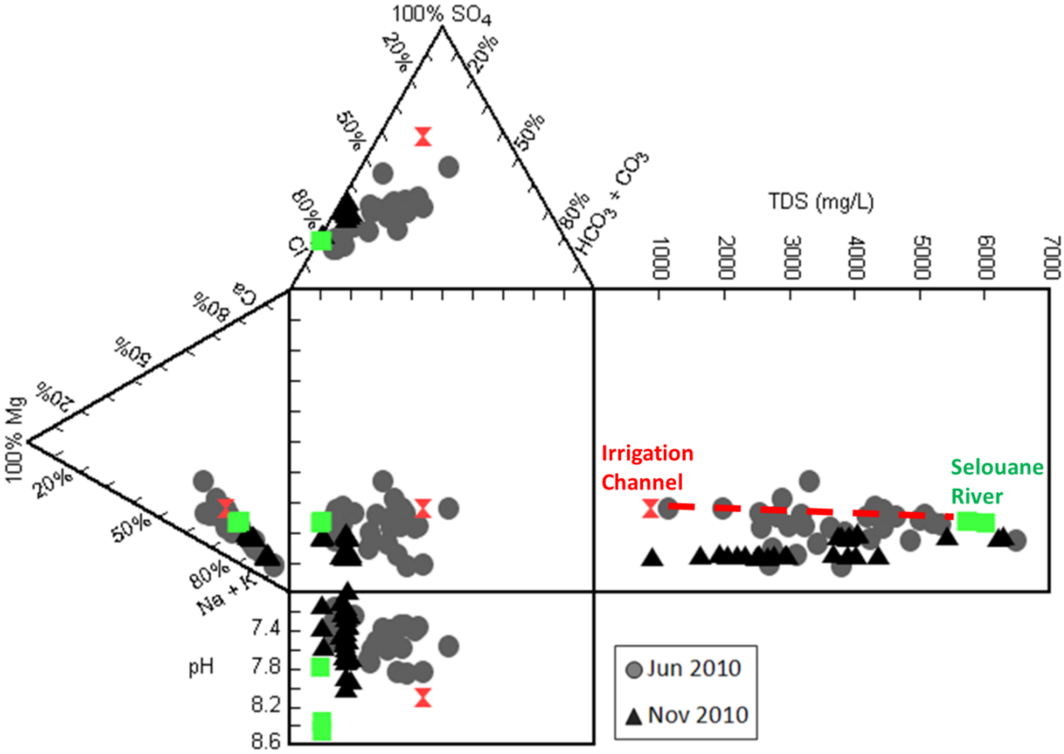

Figure 5. Durov Diagram for samples collected in June (H-IR, grey circles) and November (L-IR, black triangles) 2010 in the Bou-Areg aquifer. The red dashed line highlights the trend observed for samples in H-IR period, plotting on a line connecting the composition of the irrigation channel and the Selouane River (sampled in the L-IR period).

Figure 6
Click here to download Figure: Figure 6.docx

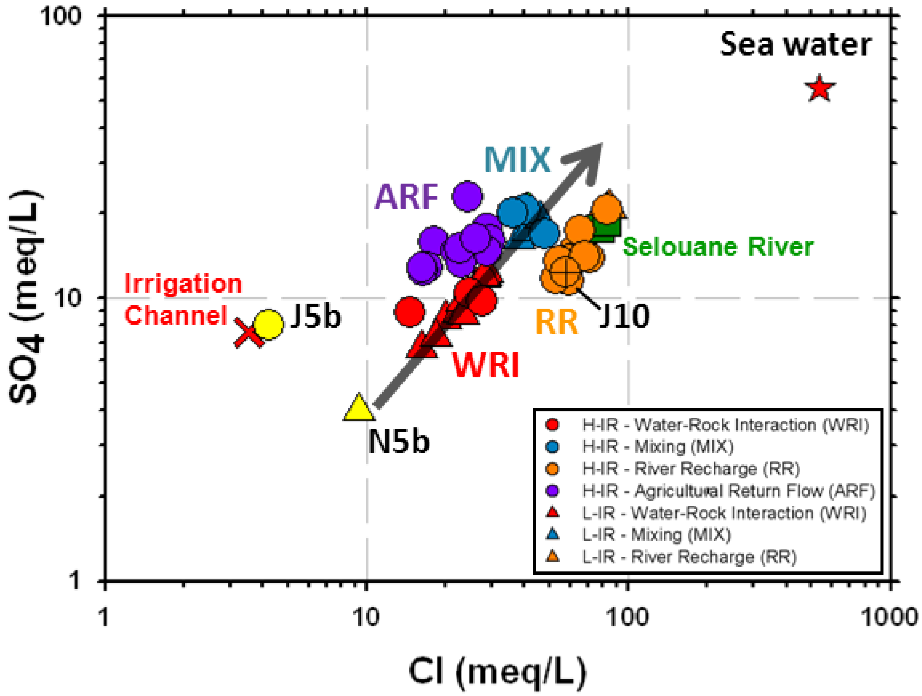

Figure 6. Plot of Cl^- vs. SO_4^{2-} for the samples collected in June (H-IR) and November (L-IR,) 2010 in the Bou-Areg aquifer. The arrow highlights the progressive change from groundwater composition dominated by WRI processes in L-IR towards a higher impact of ARF and RR in H-IR.

Figure 7

Click here to download Figure: Figure 7.docx

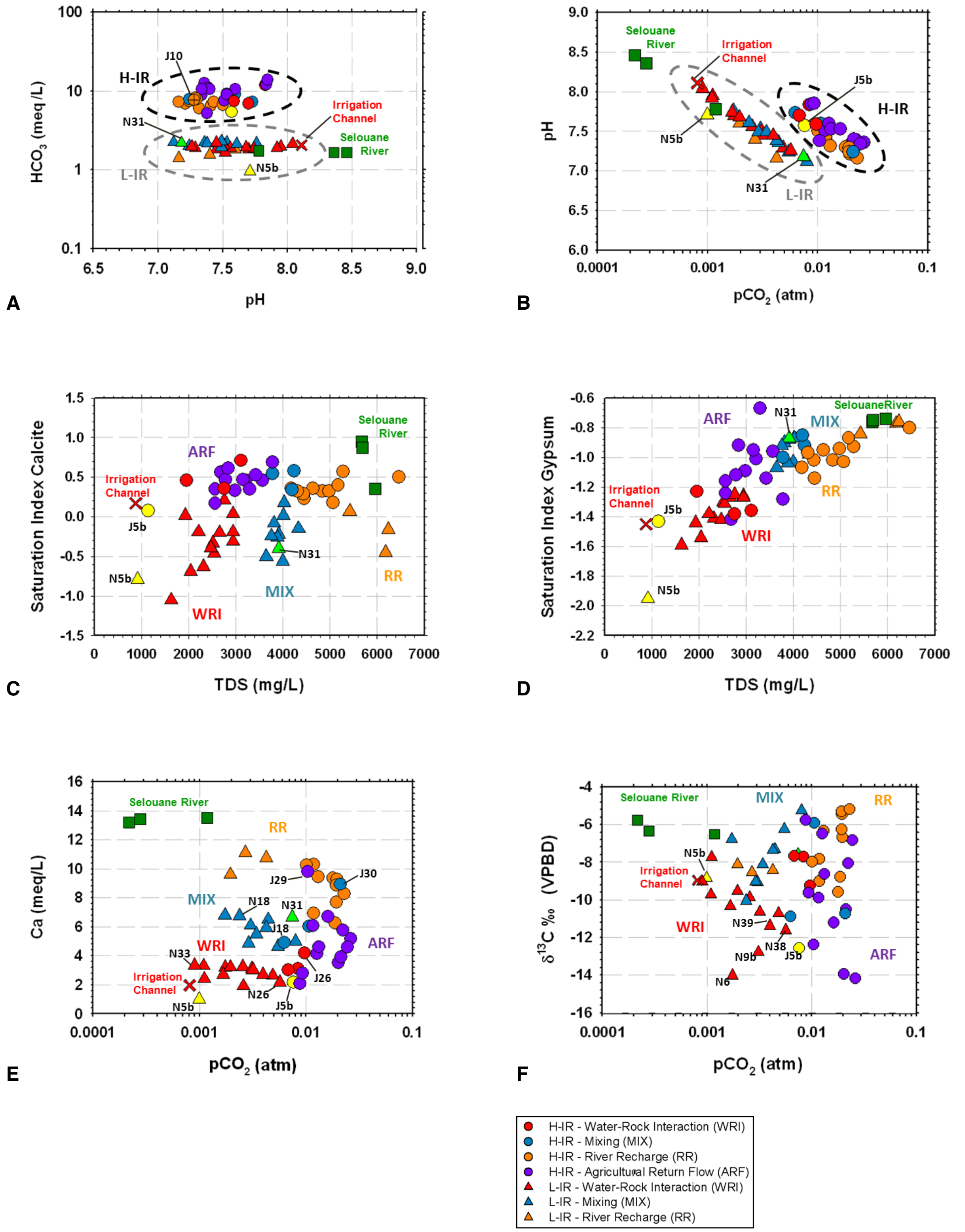

Figure 7. (A) HCO_3^- versus pH; (B) pH versus pCO_2; (C) Saturation Index of Calcite versus TDS;(D) Saturation Index of Gypsum versus TDS; (E) Calcium versus pCO_2; (F) $\delta^{13}C$ versus pCO_2 for the samples collected in in June (H-IR) and November (L-IR) 2010 in the Bou-Areg aquifer.

Figure 8

Click here to download Figure: Figure 8.docx

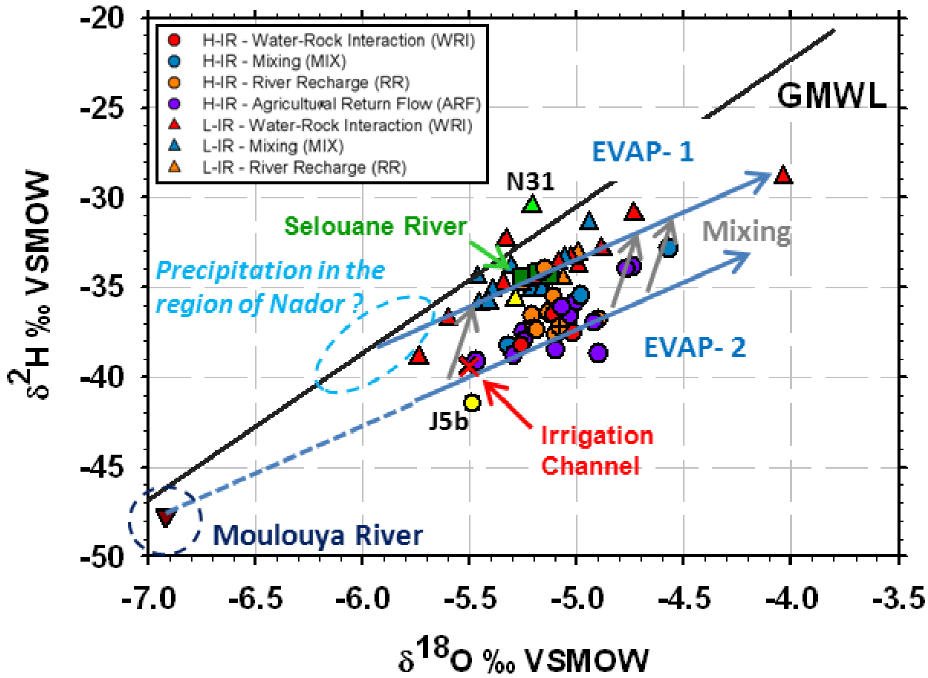

Figure 8. δ^2H D and δ^{18}O-variations in groundwater from the Bou-Areg coastal plain for June (H-IR,) and November (L-IR) 2010 in the Bou-Areg aquifer. Black line: Global Meteoric Water Line (GMWL: $\delta\ ^2H = 8.17\ \delta\ ^{18}O + 10.35$; Rozanski et al., 1993). EVAP-1 and EVAP-2 represent the evaporative trend for November and June 2010 respectively.

Figure 9

Click here to download Figure: Figure 9.docx

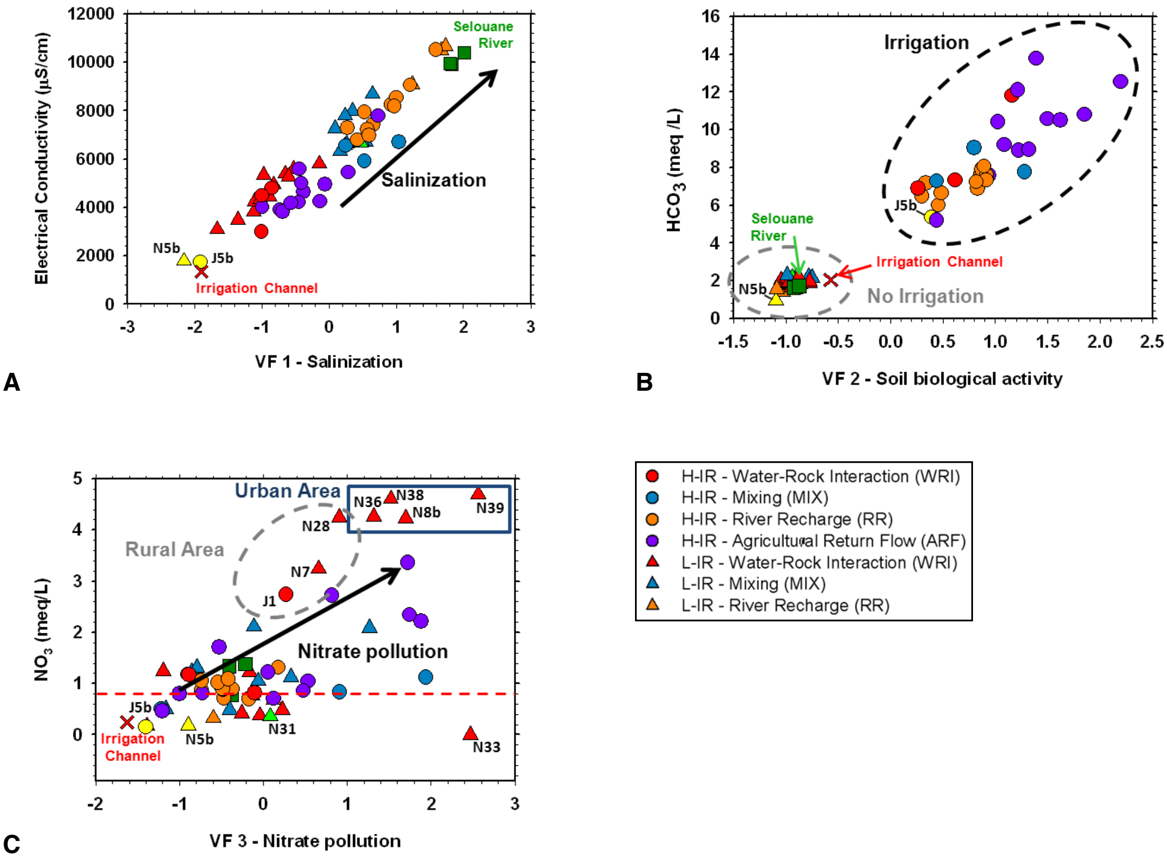

Figure 9. Relationships between varifactors (VF) and the main parameters they represent for groundwater samples collected in June (H-IR) and November (L-IR) 2010 in the Bou-Areg aquifer. (A) VF1- Salinization versus Electrical Conductivity; (B) VF2 - Soil biological activity versus HCO_3^-; (C) VF3- Nitrate pollution versus NO_3^-. The red dashed line corresponds to the WHO Drinking water standard (WHO, 2011).

Figure 10

Click here to download Figure: Figure 10.docx

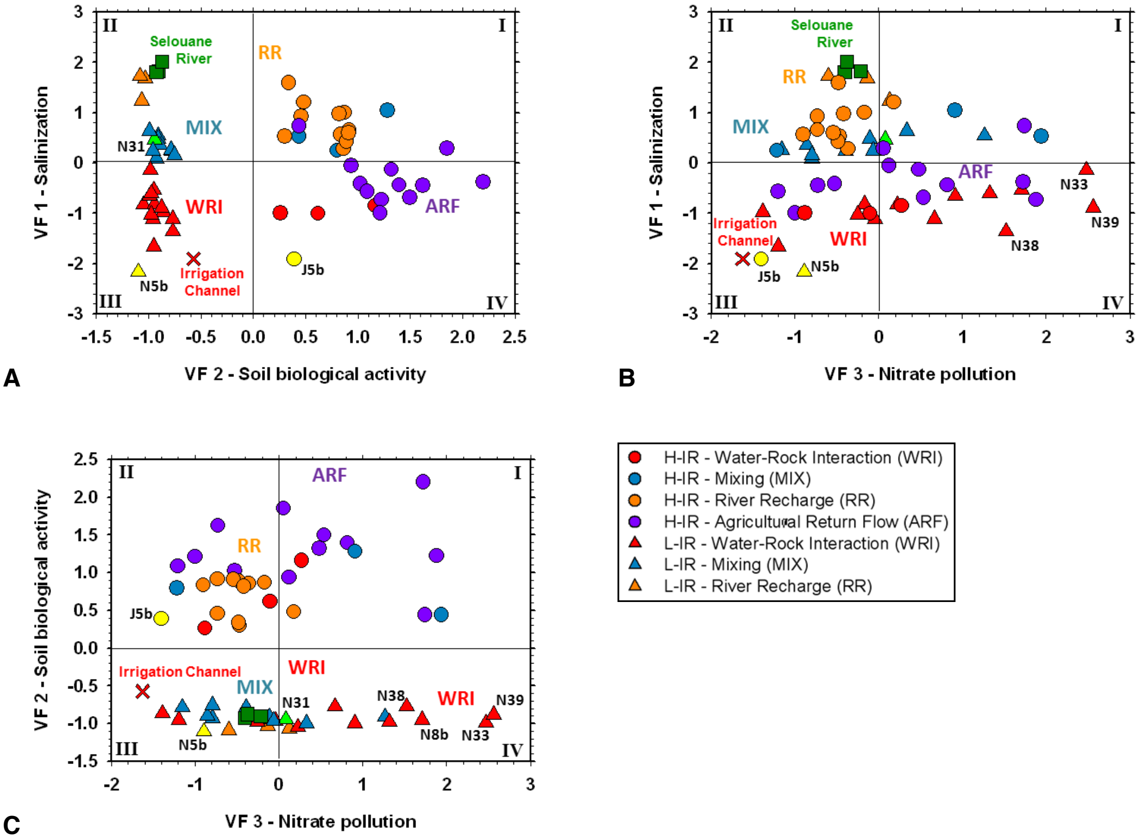

Figure 10. Distribution of the Bou-Areg groundwater samples according to their scores for VF1-aquifer salinization, VF2- soil biological activity and VF3- nitrate pollution.

Figure 11

Click here to download Figure: Figure 11.docx

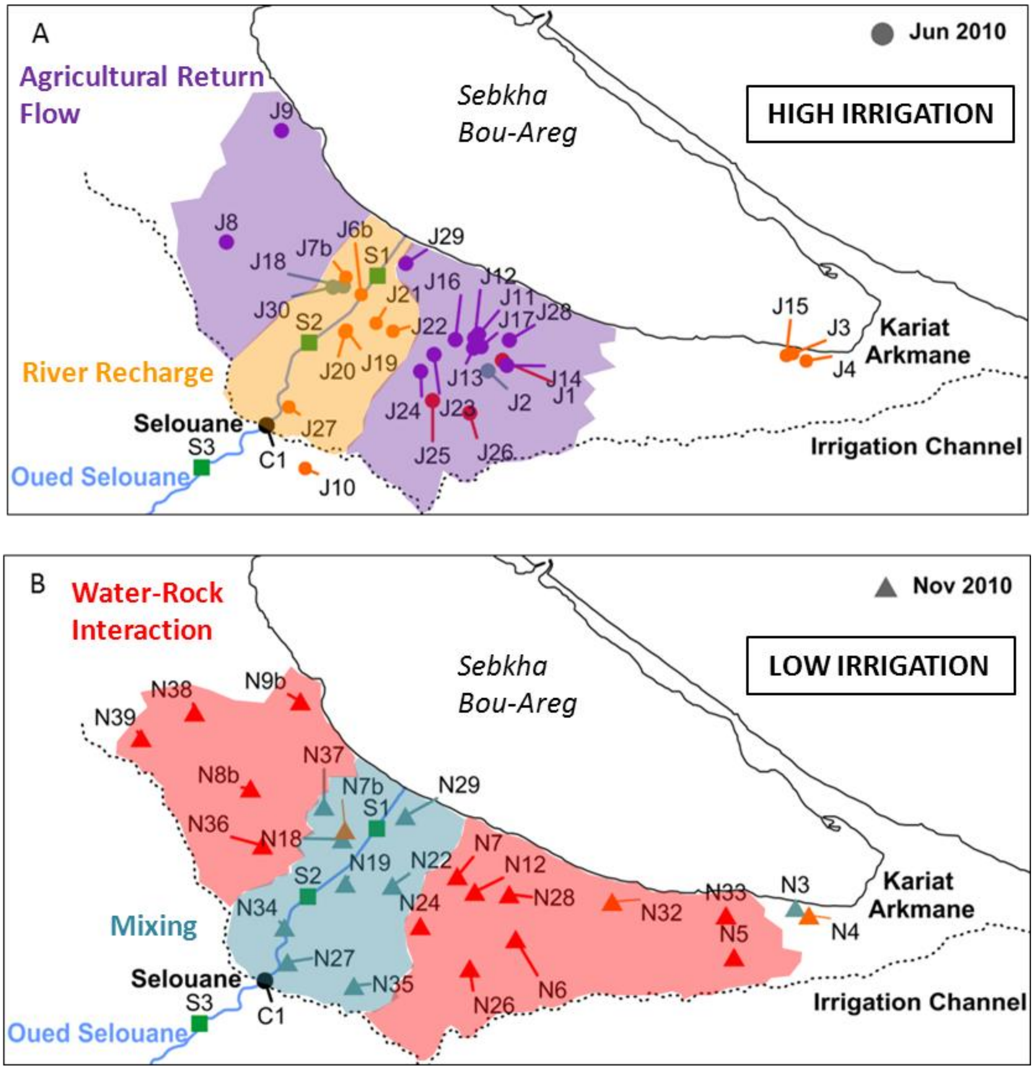

Figure 11. Seasonal variations in the Bou-Areg aquifer and impacts of agricultural activities in (A) H-IR (June 2010) and (B) L-IR (November 2010).